Preliminary results of the Muon Veto System prototype tests at U-70 IHEP, Protvino.

A.Akimenko, G.Britvich, I.Britvich, A.Filin, A.Inyakin,
I.Korolkov, L.Landsberg, V.Molchanov, V.Novikov, V.Obraztsov,
S.Petrenko, V.Polyakov, N.Smirnov, O.Tchikilev, O.Yuschenko
Institute for High Energy Physics, Protvino, Russia

V.Bolotov, S.Laptev
Institute for Nuclear Research, Moscow, Russia

P.Cooper, E.Ramberg, B.Tschirhart
Fermi National Acceleration Laboratory, Batavia, USA

1 Introduction

In November, 2000 run of U-70 we had 2 weeks of the beam time in the channel 4A to test the Muon Veto System (MVS) prototype. The main goal of the run was to demonstrate that, indeed, it is possible to achieve a high rejection for muons (better than 10^5) with a reasonable efficiency for the pions.

2 The beam

Fig.1 shows the plan of the U-70 experimental hole. The negative 4A beam is produced by primary 70 GeV protons on the Al internal target located inside the vacuum chamber inside 27-th U-70 magnetic element. The secondary beam is formed by M2 , M5, M7 dipoles and M1, M4, M6, M8, M9 quadrupoles. BS1, BS2 are $\sim$ 70 cm long iron beam-killers; K1, K2, K3, K4- 50 cm long tunable vertical and horizontal collimators.

In the MVS prototype tests the beam-line was used in three main modes:

1. The π beam:
   The M5 , M7 and K4 were tuned for 25 GeV negative particles (π^-) with $\frac{\Delta p}{p} \sim 1\%$. K1, K2, K3 were tuned to provide a narrow beam with intensity of $\sim 10^6$/spill (U-70 duty factor is 1.9/9 sec.) Both BS1 and BS2 were opened.

2. High intensity muon beam:
   M5 is tuned, as before, to 25 GeV K1, K2, BS1 are opened. BS2, K4 and K3 are closed, M7 is set to $\sim$ .7 of it's nominal value. The logic of this tuning is that 25 GeV pions decay to muons between M5 and K3 and then the pion beam is absorbed by K3, K4, BS2 and is turned out of the beam-line by M7. In turn, muons of $14 \div 20$ GeV go along the beam.

3. Low intensity muon beam:
   The magnetic elements are set as before, but all K1,K2,K3,K4, BS1, BS2 are closed. This setting provides low intensity, but clean muon beam.

3 The Muon Veto System prototype

The drawings of the MVS prototype are presented in Fig.2. The prototype consists of 27 planes of $600 \times 600 \times 41 mm^3$ steel plates interleaved with 26 scintillator planes $500 \times 480 \times 10$ mm^3. The planes are perpendicular to the beam axis, each scintillator plane consists of 12 $500 \times 40 \times 10$ mm^3 counters; two consecutive planes are arranged horizontally and vertically with a staggering in each view. All the scintillators are polished and covered with mylar. The light is read-out by PMT FEU-84(Russia) through a light guide. The signals from PMT's are sent to ADC (100 ns gate, .5pC/count, 312 channels in total). The Fig.3 illustrates the location of the MVS prototype on the beam. Elements of the ISTRA setup were used during the test: two Cerenkov's C_1, C_2 were filled with .2 atm of CO_2 to cut the low energy particles; the scintillation counters $S_1 \div S_5$ were used to define the beam, S_4 was a halo veto counter (with a hole), which was used in the anticoincidence. BPC1 $\div$ BPC2 - x and y proportional beam chambers with a step of 1mm. APC1, APC2- x,y proportional chambers with a step of 2 mm installed in front of the MVS. The magnet M1 deflects the beam in the vertical direction and was used to estimate the momentum of the beam particles. A large Veto counter (V) was used to veto the particles passing through the MVS. It consists of $500 \times 500 \times 40 mm^3$ scintillator viewed by 4 PM's.

The lead-glass counters LG0 $\div$ LG7 with the dimensions of $100 \times 100 \times 400 mm^3$ were used to provide a clean muon beam. In the high intensity muon run's LG0 $\div$ LG6 were moved into the beam; in the low intensity muon run- just LG7. The signals from LG's were sent to ADC's. MIP signals were required in LG's off-line, to suppress hadron and electron (from μ decays) background.

4 The data

The following main data sets were logged during the run:

1. High intensity muon Runs 104-107 ($\sim$ 1.6 M events):
   K1,K2, BS1-opened ; K3,K4,BS2- closed; LG0 $\div$ LG6 in the beam.
   The trigger was T=$C_1 \cdot C_2 \cdot S_1 \cdot S_2 \cdot S_3 \cdot \bar{S}_4 \cdot S_5 \cdot \bar{V}$, the rate of the monitor M=$C_1 \cdot C_2 \cdot S_1 \cdot S_2 \cdot S_3 \cdot \bar{S}_4 \cdot S_5$ was about 10^4/spill ; T/M $\sim$ 2%.

2. Low intensity muon Runs 135,136 ($\sim$ 3.6 M events):
   T=$C_1 \cdot C_2 \cdot S_1 \cdot S_2 \cdot S_3 \cdot \bar{S}_4 \cdot S_5$, the rate was $\sim 10^3$/spill. Run 136 was with LG07 in the beam line, run 135- without.

3. 25 GeV π Runs 128 $\div$ 132 (3.1 M events):
   All the collimators and BS - opened.
   T=$C_1 \cdot C_2 \cdot S_1 \cdot S_2 \cdot S_3 \cdot \bar{S}_4 \cdot S_5$, the rate was $\sim 10^5$/spill

5 Data processing

The data processing started with the calibration of the MVS: a special run with a wide muon beam with the trigger of T=$C_1 \cdot C_2 \cdot V$ was used for that. The dependence of the signal on the distance from the hit to the PM was taken into account. Fig.4(left) shows the total signal in the MVS after the calibration. The resolution of $\frac{\sigma_E}{E} = 0.15$ in perfect agreement with MC is observed. In the top figure a clear signal from the muon admixture in the hadron beam is seen. Muon disappear in the bottom figure, where the absence of the signal from V-counter was required. This muon admixture was corrected for when calculating the efficiency of the selection cuts for the pions. The muon beam momentum spectrum is presented in Fig.4(right). It is perfectly consistent with the CKM working range. A typical beam profiles are shown on Fig.5 for muon and pion beams. To clean the beam, it was required that there is just 1 hit in APC1 x,y in the square of 10×10 cm^2 around the beam and no hits outside the square. In addition the time information from the beam chambers(see Fig.6) was used to select in-time particles.

Another information used to clean the muon beam was that from the LG-counters: Fig.7 shows the LG6$\div$LG0 spectra for the high intensity muon beam and LG7 spectrum for the low intensity beam. A clear signal from 2-muon background (second peak at the double energy) is seen. For the high intensity run these class of events is enhanced due to the dead-time of the V- counter(off-time muon blocks the veto and let in-time to go through). Obvious cuts around first peak were used to suppress these events. In the low intensity beam the second peak is not seen.

After the "beam-defining" and "beam-cleaning" cuts, the main cuts which must suppress the muons with reasonable efficiency to pions were used. The first of this group of cuts, and the most obvious and efficient one is the cut on the amplitude of the V-counter. Fig.8 shows the corresponding spectra for high intensity μ, low intensity μ and π -beams. A cut of $A < 15$ counts was used. The spectra for the high intensity μ, in fact contradicts to the trigger condition ($\bar{V}$!) and is explained by the dead-time of the V-counter. A double-peak structure in the high-intensity muon spectrum is due to the drifting of the amplitude from the V counter in the beginning of the run.

To explain the logic of further cuts , Fig.9 presents x and y views of a typical 25 GeV pion event in the MVS prototype and a muon event, where muon emitted bremstrahlung photon. The numbers in the pictures are uncalibrated ADC counts(pedestal subtracted), there are 13 planes of counters in each view, 12 counters per plane. In the most of muon events clear segments of muon tracks are seen. It's look natural to introduce the following variables:

- n1- number of planes (out of 26) with just one hit above some threshold (20 ADC counts).
- n3- number of planes with more than 2 hits above the threshold.

The distributions over these variables are presented in Fig.10,12 - for the real data and in Fig.11,13 for MC Geant simulation. The following cuts were selected to suppress muons: $n1 < 9; n3 > 3$.

After these cuts, the remaining muon background mainly consists of events where muon decays in flight to $e\nu\bar{\nu}$. The decay may happen before the calorimeter or inside the calorimeter (see Fig.14). It leads to a narrow (across the beam) and relatively short (along the beam) electromagnetic shower in the MVS. To fight with this type of background, the following variables are introduced:

- $w_t = \sqrt{\frac{\sum_{i=1,12}(x_i-\bar{x})^2 \cdot E_i + \sum_{j=1,12}(y_j-\bar{y})^2 \cdot E_j}{\sum E_i + \sum E_j}}$; here x_i, y_j- is the scintillator row number for the x(y)-view; $E_i; E_j$- are the sums of energies over 13 planes for the i-th(j-th) rows of the scintillators.
- $w_{l(p)} = \sqrt{\frac{\sum_{i=1,26}(l_i-\bar{l})^2 \cdot E_i}{\sum E_i}}$; here l_i is the plane number, E_i- the sum over 12 counters in the i-th plane.

It is clear, that $w_t(w_l)$ give an estimate for the transversal(longitudinal) width of the shower in MVS. These variables are strongly effected by the noise (due to nonperfect light tightness of the calorimeter, for example). To decrease this effect, two iterations were performed, when calculating $w_{t(l)}$: in the second iteration a cut of $\pm 2 \cdot w$ around $\bar{x}; \bar{y}; \bar{l}$ was introduced when summing up.

The distributions over these variables are presented in Fig.15,17 - for the real data and in Fig.16,18 for MC Geant simulation. The following cuts were selected to suppress muons:$w_t > .55$; $w_l > 1.9 \vee w_t > 1$. The second cut is mainly against "early" muon decays before the calorimeter. As it is seen from the figures, there is a good agreement between data and MC for the muon data. There is a significant discrepancy for the w_t hadron distribution. As a result, a cut of $w_t > .8$ is removing almost all the muon background without touching pions for the MC case , but kills a lot of pions in the data. That's why a cut of $w_t > .55$ is selected. The difference can be partially explained by somewhat different algorithms of w_t calculations in MC and in the data. We'll certainly improve the situation in the nearest future.

6 The results

Table.1 shows the data reduction when applying the sequential cuts described in the previous section.

Table.1 The details of the data reduction.

Run	high int. μ	low int. μ	low int. μ, no LG	π^-
N_{read}	1595894	2654965	1065118	3139913
Beam PC cuts	309315	1480664	624489	2366359(-65448)
LG cuts	160474	1327330		
Veto<15	1799	114	176	2155952
$n_1 < 9$	1048	26	144	1951864
$n_3 > 3$	540	18	55	1951759
$w_t > .55$	265	8	18	1839404
$w_l > 1.9 \vee w_t > 1$	146	4	6	1733083
efficiency	$3.8 \cdot 10^{-6}$	$3 \cdot 10^{-6}$	$9.6 \cdot 10^{-6}$	75.3 %

In the case of the high intensity run (second column), one should take into account, first, the ratio trigger/monitor $\sim 2\%$, because the V-counter was in the trigger in the anticoincidence, and, second, the effect of the first two cuts on the monitor. The last one was determined with a special run, where V-counter was not in the trigger. The corresponding correction factor is 2.1. That is, the final efficiency for the high intensity muon run was determined as $\epsilon = \frac{146}{1595894} \times 2 \cdot 10^{-2} \times 2.1$

In other cases the efficiency calculation is straightforward. For the π run, the presence of the muon admixture in the beam was taken into account by subtracting 65448 events from 2366359 events left after the beam PC cuts. These correction was determined from the total energy spectrum of Fig.4 , where the muon signal is well seen. The muon suppression for the low intensity run without Lead Glass counters in the beam is significantly worse than that for the other runs because of the obvious reason: much more muons decay to $e\nu\bar{\nu}$ in front of the calorimeter. The effective muon decay length for the high intensity run was (see Fig.3) about 2.5 m , and 1.3 m for the low intensity run with LG7 in the beam. Instead, it was about 15 m for the run without LG.

The analogous information for the MC Geant data is presented in Table.2

Table.2 The details of the MC Geant data reduction.

Run	μ	π 25 GeV	π 12 GeV
N_{read}	2.7×10^7	10^4	10^4
Veto	18957	8356	9325
$n_1 < 9$	4219	7600	7899
$n_3 > 3$	986	7600	7510
$w_t > .8$	57	7068	6790
efficiency	$2. \cdot 10^{-6}$	70 %	68 %

As it was explained in the previous section, the w_t distributions are somewhat different for the π data and MC, that is why the cuts are different for the MC case. The effect of the Veto counter on the pions is stronger in MC, probably because the response of the V-counter is not reproduced in details (light attenuation etc.).

7 Conclusions

- The concept of the muon suppression with a fine segmented calorimeter is proved by the present experimental results.
- The structure of the calorimeter (sampling, scintillator strip width etc.) looks adequate.
- The test shows the importance of the e.m.-hadron shower separation power of the calorimeter. To insure that, ADC's must be used for the calorimeter readout rather than simple latches.
- When discussing somewhat low pion efficiency $\sim 70\%$ one should take into account, that a part of inefficiency is coming from the cut on the amplitude of the Veto counter, which is located after the calorimeter. This inefficiency can be easily removed by increase of the length of the calorimeter. Then, for 25 GeV, the pion efficiency would become 83%.
- A scan of the muon events which survived all the cuts shows that there are still some events (3-muon tracks, for example) which can be rejected with simple additional cuts. Our estimate is that the rejection can be improved by a factor of 2.
- The observed muon suppression factor of $3 \cdot 10^5$ is 3 times higher than that used in the CKM Proposal, 1998. The cuts can be reshaped to get 10^5 suppression, gaining the pion efficiency.
- There are some factors, which should lead to the stronger muon suppression in the CKM: the distance between the LG- counter and the front face of the calorimeter was(minimum) 1.3 m in the tests. This distance is important for the muon-decay background and could be reduced ,say, by a factor of 2. We did not have a precise muon momentum measurement during the tests. In CKM, momentum-dependent cuts could be used.

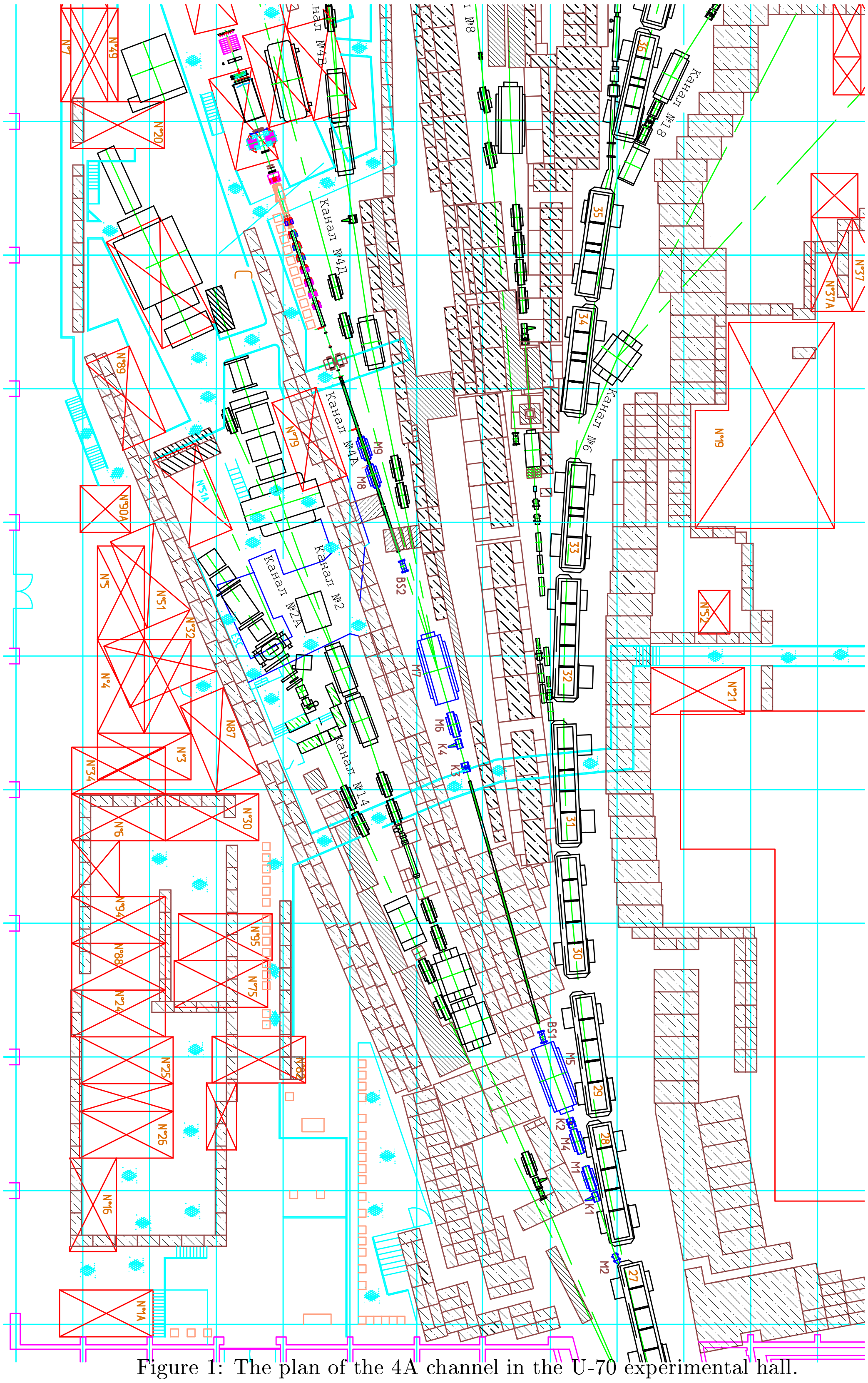

Figure 1: The plan of the 4A channel in the U-70 experimental hall.

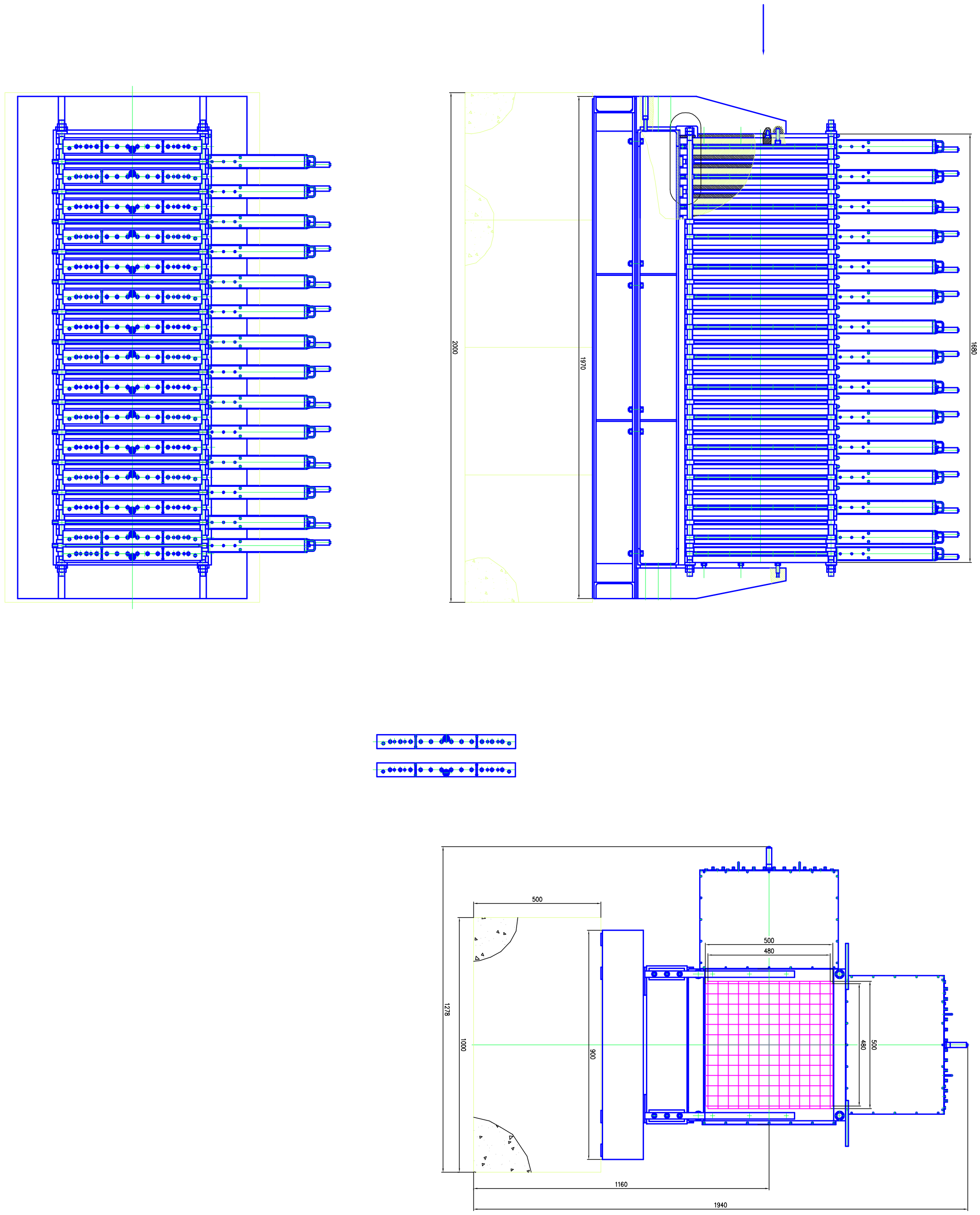

Figure 2: The MVS prototype.

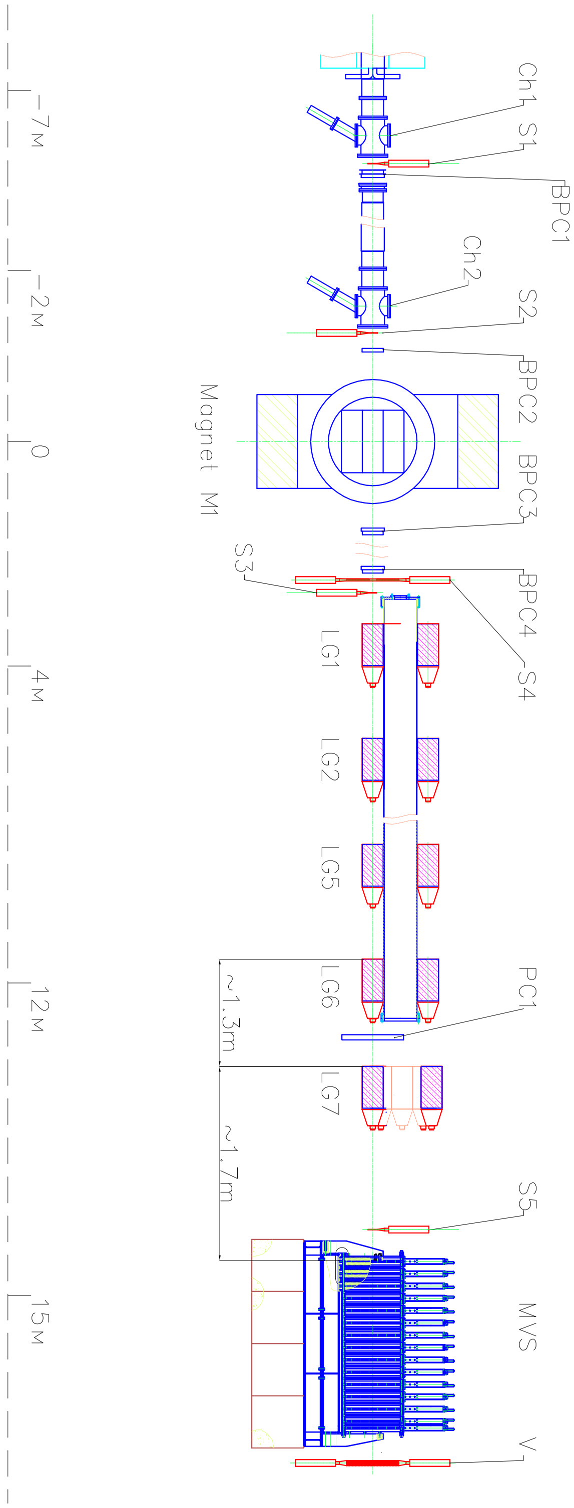

Figure 3: The MVS prototype on the ISTRA-M beam.

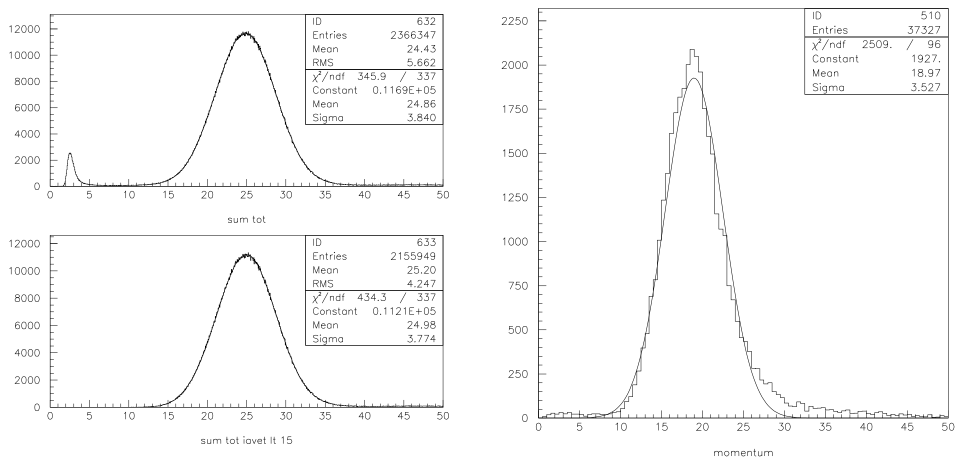

Figure 4: The total MVS signal for 25 GeV pions(left), the muon beam momentum spectrum(right).

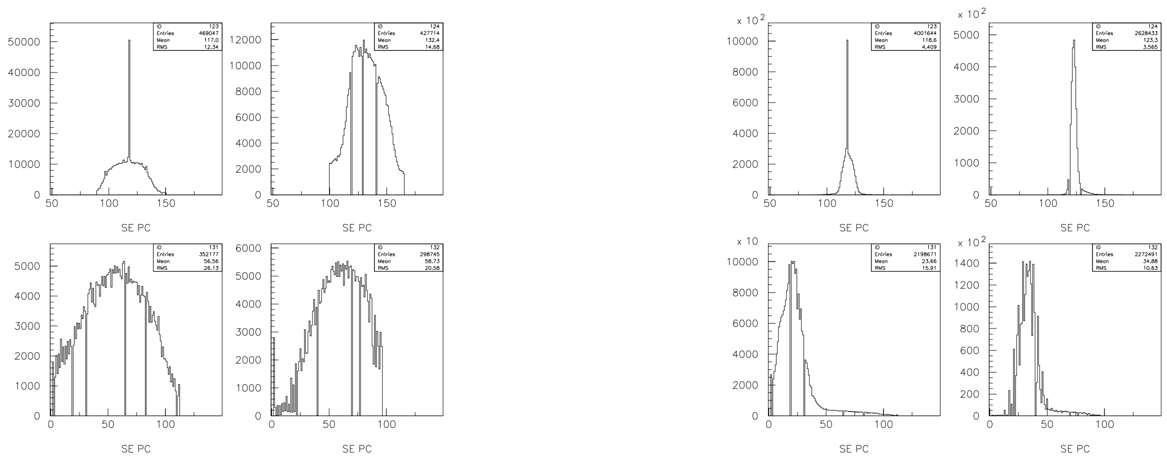

Figure 5: The beam profiles for muons(left) and pions.

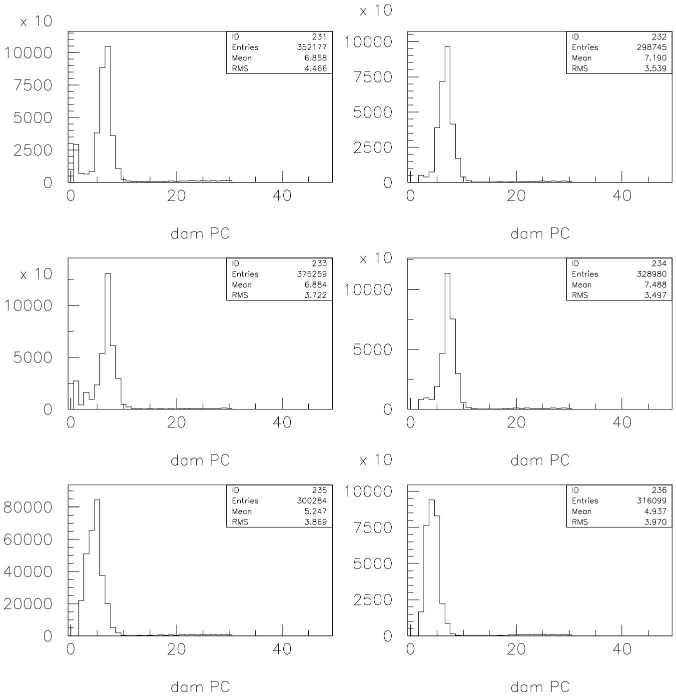

Figure 6: The time spectra from the beam PC's were used to select in-time particles.

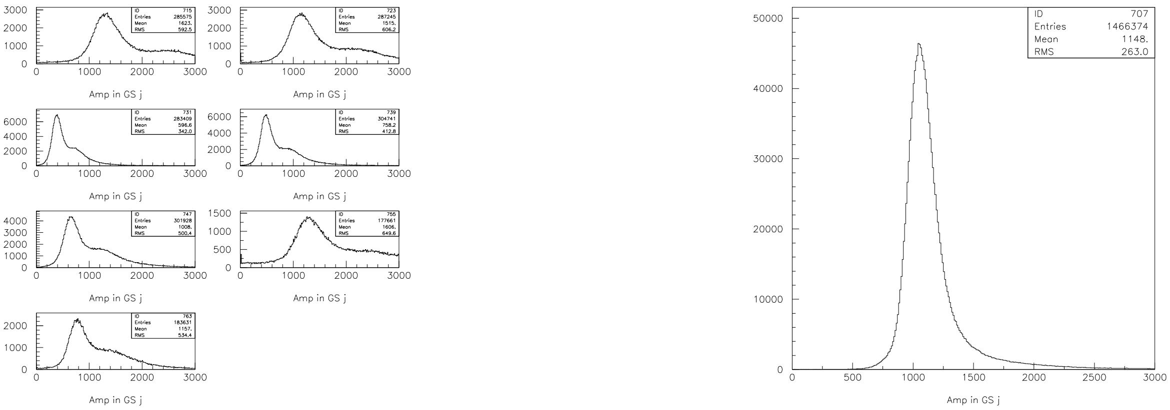

Figure 7: The signals from the LG-counters for high intensity (left) and low intensity muon runs.

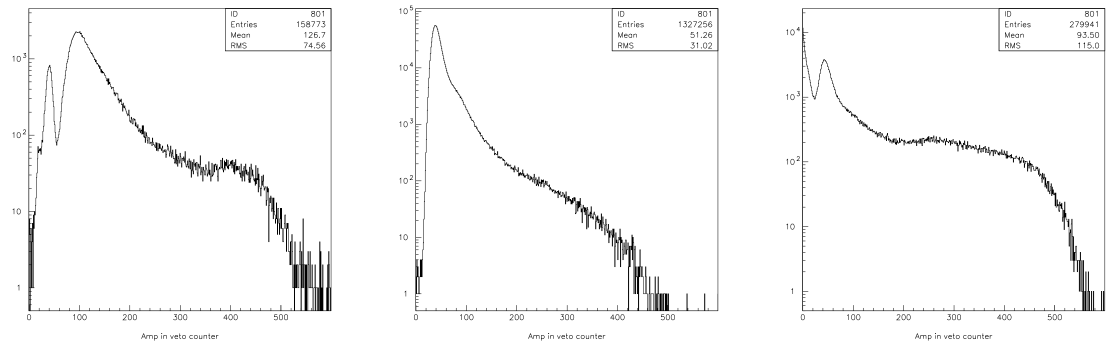

Figure 8: The amplitude from the V-counter for high intensity (left) , low intensity muon and pion runs.

Mu h: run,d,t,ev,spi=128 20001115 210704 5 1 1 1

0	0	0	0	0	0	0	0	0	0	0	0	0
0	0	105	0	0	0	0	0	0	0	0	0	0
0	0	0	10	186	0	0	0	225	69	0	0	0
0	12	40	2	630	28	0	0	0	0	0	0	0
0	651	10	316	506	78	71	94	0	0	0	0	0
1255	994	983	1180	2942	123	1046	0	3	0	0	0	0
595	840	266	2055	294	0	162	333	0	0	0	0	0
0	194	0	169	67	0	2	161	0	0	0	0	0
0	44	0	680	31	236	0	32	0	0	0	0	0
0	0	0	0	0	121	0	0	35	0	0	0	0
0	1	0	0	0	241	0	0	0	0	0	0	0
0	0	0	700	24	0	0	0	0	0	0	0	0

Mu vert.

40	143	0	709	0	0	0	0	0	0	0	0	0
0	0	0	1	0	0	0	0	0	0	0	0	0
0	0	0	0	0	0	0	0	0	0	0	0	0
7	0	0	142	0	0	0	0	0	0	0	3	0
4	15	159	0	0	162	0	0	281	0	0	0	0
12	0	15	666	5	3	211	377	0	0	0	0	0
1324	480	353	429	117	120	0	0	0	0	0	0	0
1417	466	1408	1265	187	0	1949	0	0	0	0	5	0
6	0	435	225	400	35	0	0	0	0	0	0	0
0	0	214	537	212	71	93	0	0	0	0	3	0
2	17	0	0	0	0	438	94	0	0	0	0	0
0	0	0	0	0	0	0	0	0	0	0	0	0

Mu h: run,d,t,ev,spi=135 20001116 151432 1639109 882 7 8 396

0	6	0	0	0	0	0	0	0	0	0	0	0
94	4	0	0	0	0	0	0	0	0	0	0	0
0	9	4	5	0	0	0	0	0	0	0	0	0
0	59	14	20	0	0	0	0	0	0	0	0	0
897	246	142	7	0	0	0	0	0	0	0	0	0
1520	0	377	187	65	45	144	0	0	0	0	0	0
47	97	6	48	0	0	0	357	116	3	0	0	0
0	11	4	2	0	0	0	0	0	55	53	0	0
0	0	0	0	0	0	0	0	0	0	0	24	0
0	0	0	0	0	0	0	0	0	0	0	0	0
0	15	0	0	0	0	0	0	0	0	0	0	0
0	9	51	0	0	0	0	0	0	0	0	0	0

Mu ver

1	0	0	0	0	0	0	0	0	0	0	0	0
0	11	0	0	0	0	0	0	0	0	0	0	0
9	76	0	0	0	0	0	0	0	0	0	0	0
19	0	0	0	0	0	0	0	0	0	0	0	0
4	9	2	0	0	0	0	0	0	0	0	1	0
96	80	123	51	52	96	49	0	0	0	0	0	0
1827	1557	114	3	0	0	0	34	42	227	105	371	0
615	1091	157	66	0	0	0	0	0	0	0	0	0
8	25	2	0	0	0	0	0	0	0	0	0	0
8	6	0	171	0	0	0	0	0	0	0	0	0
6	0	2	0	0	0	0	0	0	0	0	0	0
10	0	0	0	0	0	0	0	0	0	0	0	0

Figure 9: x (top) and y view of 25 GeV π event (left) and muon event(right) in the MVS

Figure 10: The distribution over n1 variable for the low intensity muon run (left) and pion run.

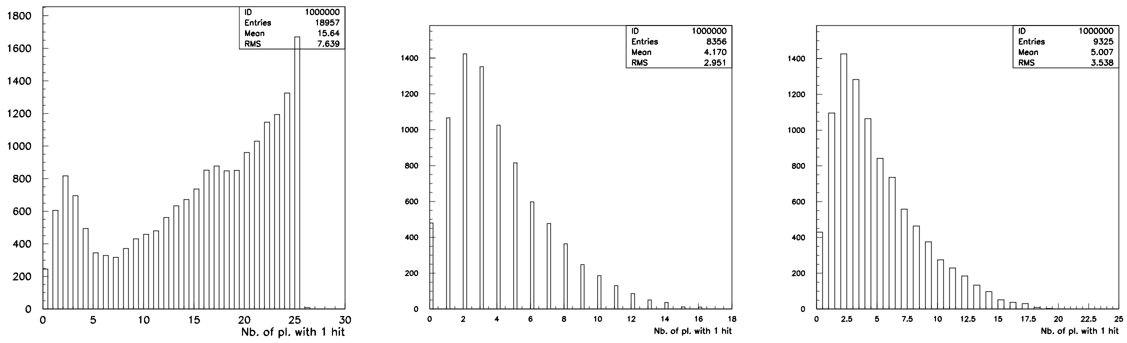

Figure 11: The distribution over n1 variable for the Geant MC: muons(left), 25 GeV pions, 12 GeV pions(right)

Figure 12: The distribution over n3 variable for the low intensity muon run (left) and pion run.

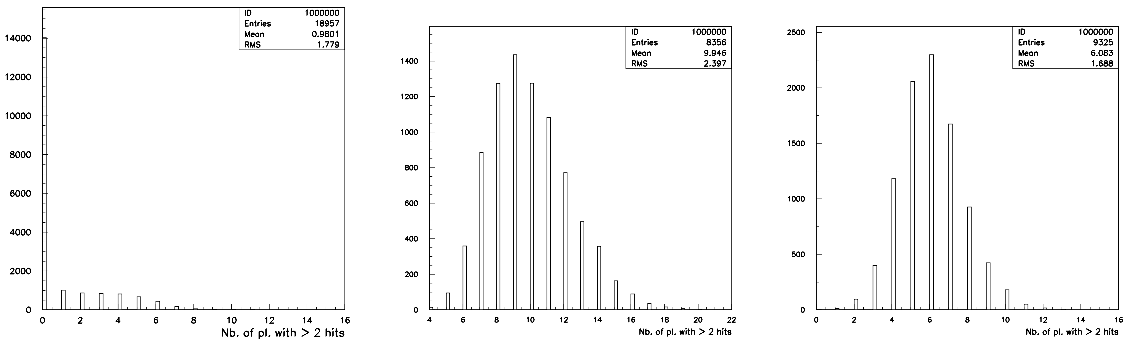

Figure 13: The distribution over n3 variable for the Geant MC: muons(left), 25 GeV pions, 12 GeV pions(right)

Mu h: run,d,t,ev,spi=135 20001116 185630 3041724 2245 6 7 18

0	5	0	0	0	0	0	0	0	0	0	0	0
0	3	0	0	0	0	0	0	0	0	0	0	0
0	3	0	0	0	1	0	0	0	0	0	0	0
0	0	0	0	0	0	0	0	0	0	0	0	0
0	12	0	13	0	0	0	0	0	0	0	0	0
0	16	0	63	0	0	0	0	0	0	0	0	0
4	164	153	58	20	0	0	0	0	0	0	0	0
16	1714	1658	260	454	0	0	0	0	0	0	0	0
0	6	215	7	1	0	0	0	0	0	0	0	0
0	12	29	0	0	0	0	0	0	0	0	0	0
0	0	0	0	0	0	0	0	0	0	0	0	0
0	15	0	0	0	0	0	0	0	0	0	0	0

Mu ver

0	0	0	0	45	0	0	0	0	0	0	0	0
0	0	0	0	0	0	0	0	0	0	0	0	0
0	0	0	0	0	0	0	0	0	0	0	1	0
0	0	0	0	0	0	0	0	0	0	0	0	0
0	12	0	18	0	0	0	0	0	0	0	2	0
8	71	35	17	0	0	0	0	0	0	0	1	0
16	296	141	4	0	0	0	0	0	0	0	3	0
1367	1720	657	159	0	0	0	0	0	0	0	3	0
16	91	55	114	0	0	0	0	0	0	0	0	0
4	0	1	0	0	0	0	0	0	0	0	3	0
5	0	2	0	0	0	0	0	0	0	0	4	0
3	0	0	0	0	0	0	0	0	0	0	1	0

Mu h: run,d,t,ev,spi=135 20001116 170253 2301693 1547 6 7 0

0	0	0	0	0	0	0	0	0	0	0	0	0
0	0	0	0	0	0	0	0	0	0	0	0	0
0	0	0	0	0	1	0	0	0	0	0	0	0
0	0	13	0	0	1	0	0	0	0	0	0	0
0	0	0	0	0	0	15	0	0	0	0	0	0
0	0	0	0	7	64	82	12	0	0	0	0	0
144	139	46	35	1763	483	309	612	0	0	0	0	0
0	0	0	2	58	165	167	229	0	32	0	0	0
0	0	9	0	16	0	27	8	0	0	0	0	0
0	0	0	0	53	0	0	0	0	0	0	0	0
0	0	0	0	0	0	2	0	0	0	0	0	0
0	0	0	0	0	8	0	0	0	0	0	0	0

Mu ver

0	0	0	0	0	0	0	0	0	0	0	0	0
0	0	0	0	0	7	0	0	0	0	0	0	0
0	0	0	0	0	8	0	13	0	0	0	0	0
0	0	0	0	0	18	0	0	0	4	0	0	0
0	0	0	0	114	92	214	27	0	0	0	0	0
0	0	0	20	646	1815	377	0	0	0	0	0	0
75	78	34	262	335	1495	0	0	0	0	0	0	0
0	0	0	0	10	23	68	0	0	0	0	0	0
0	0	0	0	0	0	0	15	0	0	0	0	0
0	0	0	0	0	11	0	0	0	0	0	0	0
0	0	0	0	0	63	0	0	0	0	0	0	0
0	0	0	0	0	9	0	0	0	0	0	0	0

Figure 14: x and y view of the e.m. shower caused by $\mu \to e\nu\bar{\nu}$ decay before the calorimeter(left) or inside.(low intensity muon run)

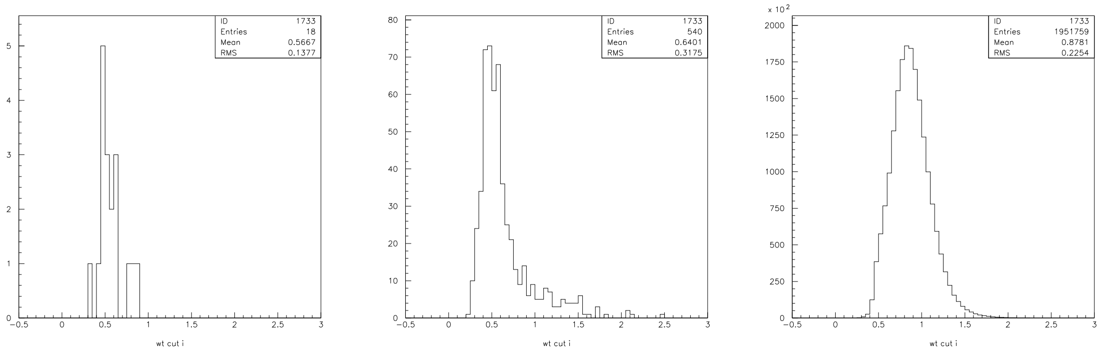

Figure 15: The distribution over w_t variable for the low intensity(left), high intensity muon runs and the 25 GeV pion run.

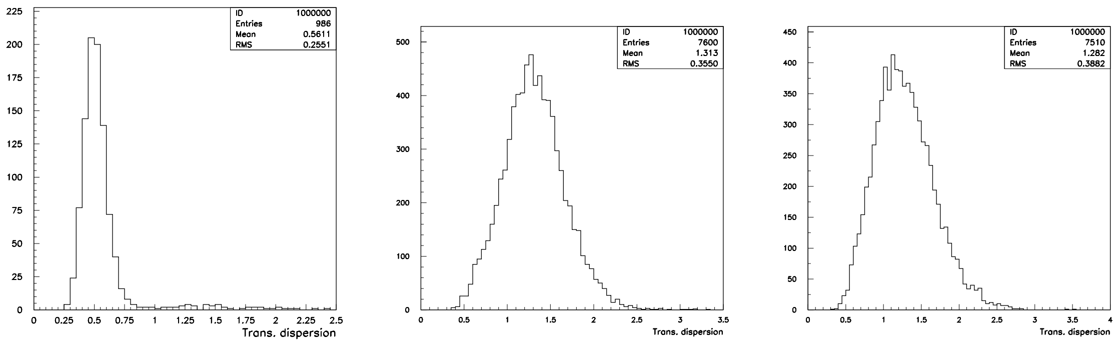

Figure 16: The distribution over w_t variable for the Geant MC: muons(left), 25 GeV pions, 12 GeV pions(right)

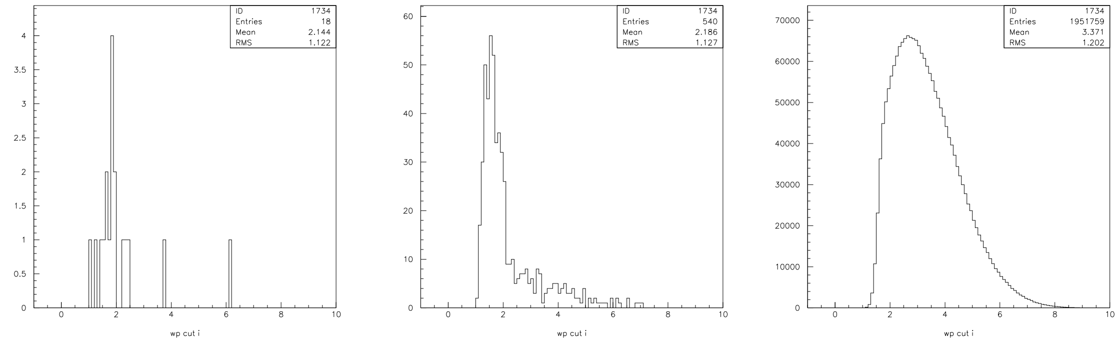

Figure 17: The distribution over w_l variable for the high intensity(left), high intensity muon runs and the 25 GeV pion run.

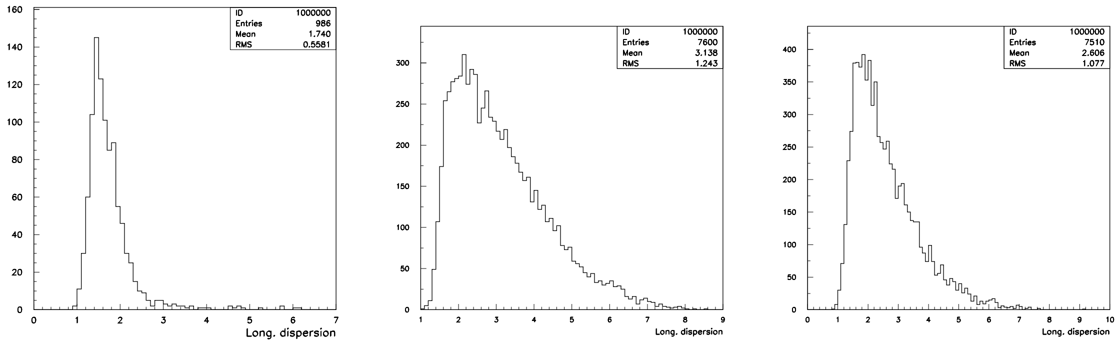

Figure 18: The distribution over w_l variable for the Geant MC: muons(left), 25 GeV pions, 12 GeV pions(right)